EINDHOVEN UNIVERSITY OF TECHNOLOGY

Chemical boundary layers in CVD II. Reversible reactions

Citation for published version (APA):
Croon, de, M. H. J. M., & Giling, L. J. (1990). Chemical boundary layers in CVD II. Reversible reactions. *Journal of the Electrochemical Society*, *137*(11), 3606-3612. https://doi.org/10.1149/1.2086276

DOI:
10.1149/1.2086276

Document status and date:
Published: 01/01/1990

Document Version:
Publisher's PDF, also known as Version of Record (includes final page, issue and volume numbers)

Please check the document version of this publication:

• A submitted manuscript is the version of the article upon submission and before peer-review. There can be important differences between the submitted version and the official published version of record. People interested in the research are advised to contact the author for the final version of the publication, or visit the DOI to the publisher's website.
• The final author version and the galley proof are versions of the publication after peer review.
• The final published version features the final layout of the paper including the volume, issue and page numbers.

Link to publication

General rights
Copyright and moral rights for the publications made accessible in the public portal are retained by the authors and/or other copyright owners and it is a condition of accessing publications that users recognise and abide by the legal requirements associated with these rights.

• Users may download and print one copy of any publication from the public portal for the purpose of private study or research.
• You may not further distribute the material or use it for any profit-making activity or commercial gain
• You may freely distribute the URL identifying the publication in the public portal.

If the publication is distributed under the terms of Article 25fa of the Dutch Copyright Act, indicated by the "Taverne" license above, please follow below link for the End User Agreement:

www.tue.nl/taverne

Take down policy
If you believe that this document breaches copyright please contact us at:

openaccess@tue.nl

providing details and we will investigate your claim.

Download date: 07. Jun. 2023

i.) Liquid methanol produces a physisorbed layer at the gallium arsenide surface. The layer is non-protective and can persist for hours following evaporation of the liquid. Because the physisorbed methanol layer is non-protective, the natural oxide re-grows while methanol is still adsorbed on the surface.

ii.) The natural oxide of gallium arsenide contains Ga_2O_3 as well as a non-stoichiometric sub-oxide of gallium or arsenic. Liquid methanol treatment removes the sub-oxide component of the surface layer. It may remove surface Ga_2O_3 to a lesser extent as well.

iii.) Methoxide ion in solution (formed when KOH is dissolved in methanol) appears to etch the gallium arsenide surface via a two-step oxidation/dissolution process.

All of these conclusions carry implications for semiconductor processing, particularly for solvent cleaning and degreasing steps. In addition, it has been demonstrated that surface infrared spectroscopy is a sensitive technique of investigation and is capable of monitoring minute changes (down to the monolayer level) in surface films at liquid-solid interfaces.

Acknowledgements

The authors would like to thank Y. J. Chabal and S. B. Christman of AT&T Bell Laboratories for important technical advice and useful discussions. They also thank J. M. Fountain and J. Yota for experimental assistance. Portions of this work have been supported by the National Science Foundation (Grant No. DMR 87-08153), the Engineering Foundation (Grant No. RI-A-87-9), and the Arizona State University Graduate Student Association Research Development Program.

REFERENCES

1. K. E. Bean in "Semiconductor Materials and Process Technology Handbook," G. E. McGuire, Editor, Ch. 4, Noyes Publications, Park Ridge, NJ (1988).
2. S. W. Ghandhi, "VLSI Fabrication Principles," p. 523, John Wiley and Sons, New York (1983).
3. C. W. Fischer and J. D. Canaday, *This Journal*, **129**, 1016 (1982).
4. F. M. Hoffman, *Surf. Sci. Reports*, **3**, 1 (1983).
5. Y. J. Chabal, *ibid.*, **8**, 211 (1988).
6. V. A. Burrows, S. Sundaresan, Y. J. Chabal, and S. B. Christman, *Surf. Sci.*, **160**, 122 (1985).
7. V. A. Burrows, *J. Electron Spectrosc. Relat. Phenom.*, **45**, 41 (1987).
8. Y. J. Chabal and K. Raghavachari, *Phys. Rev. Lett.*, **53**, 282 (1984).
9. V. A. Burrows, Y. J. Chabal, G. S. Higashi, K. Raghavachari, and S. B. Christman, *Appl. Phys. Lett.*, **53**, 998 (1988).
10. Y. J. Chabal, G. S. Higashi, K. Raghavachari, and V. A. Burrows, *J. Vac. Sci. Technol. A*, **7**, 2104 (1989).
11. S. Pons, *J. Electron Spectrosc. Relat. Phenom.*, **45**, 303 (1987).
12. N. J. Harrick, "Internal Reflection Spectroscopy," p. 141, Harrick Scientific Corporation Ossining, NY (1967).
13. C. M. Wolfe, N. Holonyak, Jr., and G. E. Stillman, "Physical Properties of Semiconductors," p. 204, Prentice Hall, Englewood Cliffs, NJ (1989).
14. M. Born and E. Wolf, "Principles of Optics, pp. 47-48, Pergamon Press, Oxford (1980).
15. M. Falk and E. Whalley, *J. Chem. Phys.*, **34**, 1554 (1961).
16. A. C. Adams and B. Pruniaux, *This Journal*, **120**, 408 (1973).
17. G. Herzberg, "Molecular Spectra and Molecular Structure," Vol. 1, p. 528, D. Van Nostrand Company, Princeton, NJ (1950).
18. F. A. Miller, G. L. Carlson, F. F. Bentley, and W. H. Jones, *Spectrochim. Acta*, **16**, 195 (1960).
19. B. Schwartz, *CRC Crit. Rev. Solid State Sci.*, **5**, 609 (1975).
20. N. T. McDevitt and W. L. Baum, *Spectrochim. Acta*, **20**, 799 (1964).
21. R. C. Weast, Editor, "The CRC Handbook of Chemistry and Physics," B-94, CRC Press, Boca Raton, FL (1983).
22. H. Stephen and T. Stephen, "Solubilities of Inorganic and Organic Compounds," p. 927, Pergamon Press, NY (1963).
23. F. Lukes, *Surf. Sci.*, **30**, 91 (1972).
24. K. Nakamoto, "Infrared and Raman Spectra of Inorganic and Coordination Compounds," p. 122, John Wiley and Sons, New York (1978).
25. A. Unmack, *Z. Phys. Chem.*, **133**, 45 (1928).
26. E. F. Caldin and G. Long, *J. Chem. Soc.*, 3737 (1954).
27. C. J. Pouchert, Editor, "The Aldrich Library of Infrared Spectra," p. 1556, Aldrich Chemical Company, Milwaukee, WI (1981).
28. N. J. Harrick, "Internal Reflection Spectroscopy," p. 27, Harrick Scientific Corp., Ossining, NY (1967).
29. B. Schwartz, *This Journal*, **118**, 657 (1971).
30. M. E. Straumanis, J. P. Krumme, and W. J. James, *ibid.*, **115**, 1050 (1968).

Chemical Boundary Layers in CVD

II. Reversible Reactions

M. H. J. M. de Croon and L. J. Giling

Department of Experimental Solid State Physics III, R.I.M., Faculty of Science, University of Nijmegen, 6525 ED Nijmegen, The Netherlands

ABSTRACT

In addition to irreversible reactions, which were treated in part I, reversible reactions in the gas phase have been studied using the concept of the chemical boundary layer. The analysis is given for the situations in which either the forward or the back reaction is dominant. Two conceptual models for the boundary layer are used in the calculations: the block model and the linearly varying k model. It is shown that both models lead to the same deposition rates.

One of the important processes available for the growth of both electronically active and insulating layers is chemical vapor deposition (CVD). Studies in connection with this technique until recently mainly have dealt with growth and doping, *i.e.*, with the practical technology of the process. The theoretical modeling of the physical phenomena occurring in CVD reactors, such as flow dynamics and depletion effects, appears to be difficult, but already several attempts have been made and understanding in this area is growing rapidly, too (1-5). However, the chemical aspects of the CVD process up until now are mostly poorly understood, and the chemistry underlying the growth still constitutes a field full of speculations. When the chemistry is coupled to the flow dynamics of the process, an even more complicated situation arises. Numerical methods have been used to solve the differential equations which mathematically describe this problem (1-4). Necessarily the results then are given in graphical form, rather than analytically. Although the graphical representation of results obtained by the simulations is probably

very quantitative and also quite instructive, we think that the exactness is obtained at the expense of a loss of direct insight into the physics and chemistry of the process. For this reason we follow another, semi-quantitative but analytical route to describe the chemical/physical behavior.

Recently (6, 7) we developed an analytical, two-dimensional model in which flow, diffusion, and thermal diffusion of growth species and surface kinetics were combined in order to predict deposition rates and depletion effects in a horizontal reactor at atmospheric pressure in the diffusion-limited and surface reaction-controlled regime. If one considers not only gas phase transport of growth species to the substrate surface together with reaction at this surface, but also homogeneous reaction kinetics in the CVD system, then the description becomes more realistic. However, because of the presence of steep temperature gradients in the reactor, in general gas phase reactions will be very strong functions of the position in the reactor. Therefore a complete analytical solution of this problem is impossible, but still rather good approximations can be found which give an accurate description of the growth process within the uncertainties of the experiment itself.

In part I of this series (8) we introduced this approximate solution to the problem in order to describe the deposition rate in a CVD reactor. The solution was based on the notion of a chemical boundary layer, a conceptual region in the reactor caused, not by developing velocity and temperature fields, but by the chemistry of the process itself, coupled to the temperature profile in the reactor. Up until now we only presented an analysis for the case of unidirectional homogeneous gas phase reactions of arbitrary reaction order. In this paper we will extend our analysis to the case of reversible reactions in the gas phase.

The Reactor System

Our analysis is based on a two-dimensional reactor system with constant height (h) and with a long horizontal susceptor. Cartesian coordinates are used where x is in the flow direction and y is in the direction perpendicular to the substrate. Flow conditions are supposed to be laminar; in addition, a steep temperature gradient is imposed between hot susceptor, $T = T_s$, and cooled upper wall. The temperature of this upper wall is taken to be equal to the inlet temperature of the gases, T_0. Reactant concentrations are assumed to be small if compared to the concentration of the carrier gas. Transport in the flow direction is considered to be completely dominated by forced flow. End effects are not taken into account, thus the profiles of velocity and temperature are completely developed. This will be true after a thermal entrance length, x_T, which for practical reactors is a distance of several to tens of centimeters. The concentration entrance length, x_c, defined by the distance necessary to develop the concentration profile by diffusion and thermal diffusion in a laminar flow, at most will be as large as the thermal entrance length, as is shown by van de Ven (9). Therefore concentration profiles also will be considered as completely developed. For this case, as shown in part I, the temperature distribution in the gas phase is described by the relation

$$T(y) = [T_s^{1+\beta} - (T_s^{1+\beta} - T_0^{1+\beta})y/h]^{\frac{1}{1+\beta}} \quad [1]$$

where β equals the temperature dependence of the thermal conductivity of the carrier gas, which is about equal to 0.7 (3, 10). The velocity profile $v_x(y)$ in this configuration appears to be a distorted parabola with its maximum shifted slightly towards the colder part of the reactor. A schematic overview of the CVD reactor system that we will use for our analysis is given in Fig. 1.

In this context we suppose that film growth proceeds through a gas phase reaction followed by adsorption of products. Finally we assume—for the sake of computational simplicity—that the reactants of the forward gas phase reaction have sticking coefficient zero, whereas products of this reaction will adsorb on the hot substrate but not on the cold upper wall of the reactor. This adsorption will give rise to deposition on (or growth of) the substrate material.

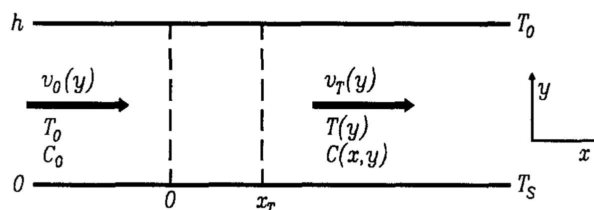

Fig. 1. Schematic model of the reactor used in the calculations

Analysis and Discussion

The model which was described in part I allowed us to calculate deposition rates in horizontal CVD reactors for the case in which the deposition process is limited by a highly activated unidirectional chemical reaction in the gas phase, *viz.*

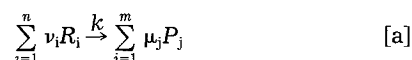

$$\sum_{i=1}^{n} \nu_i R_i \xrightarrow{k} \sum_{j=1}^{m} \mu_j P_j \quad [a]$$

in which R_i are reactants and P_j products. The main idea behind the model was the notion of a chemical reaction boundary layer, *i.e.*, a conceptual layer in the reactor just above the hot susceptor where the chemical reaction takes place. This layer results from the coupling between the strong temperature dependence of chemical rate constant and the steep, imposed temperature gradient in the reactor.

It was found (Eq. 23 and 25 in part I) that an expression could be derived relating the width of the reaction boundary layer to parameters defining the temperature gradient in the reactor and to the apparent activation energy of the reaction, E_a, by solving Eq. [2]

$$\int_0^h k \prod_{l=1}^{n} [R_l]^{\nu_l}\, dy = k_{T_s} \left(\prod_{l=1}^{n} [R_{l,T_s}]^{\nu_l} \right) \delta \quad [2]$$

where k equals the reaction rate constant, k_{T_s} its value at temperature T_s, $[R_l]$ equals the concentration of reaction R_l, $[R_{l,T_s}]$ the magnitude of the latter at temperature T_s, *i.e.*, close to the susceptor surface, and ν_l the fractional reaction order with respect to compound R_l. The thickness of this chemical boundary later, δ, is given by

$$\frac{\delta}{h} = \frac{(1+\beta)\left(\dfrac{T_s}{T_0}\right)^{1+\beta}}{\left(\dfrac{T_s}{T_0}\right)^{1+\beta} - 1} \cdot \frac{RT_s}{E_a} \quad [3]$$

showing that in good approximation it is independent of the partial order of reaction, ν_l, and of the concentration of the reactants.

From its definition as given by Eq. [2], it can be seen that the concentration gradient can be thought of as totally confined to a boundary layer. The form of the boundary layer, however, is not defined and will depend on our interpretation of the right-hand side of Eq. [2]. As was shown in (8), in principle an infinite number of, but for practical analytical solutions two, models emerge from our analysis. The first and simplest model, see Fig. 2, interprets the reaction boundary layer as a zone of constant width δ where the temperature, T_s, is constant. Consequently also the reaction rate constant, k_{T_s}, has a constant value (block model). In the second model it is assumed that the reaction rate constant is a linear function of height in a boundary layer of width 2δ, as shown in Fig. 3, whereas the temperature in this layer is taken as (approximately) constant. In this model, also, the reaction occurs in a boundary layer but, because of the linearly varying rate constant, the reaction rate is more concentrated near the susceptor surface.

In this study we preferably will make use of the first model because of the mathematical simplicity. However, below it will be shown that in practice both models lead to nearly the same deposition rates. One has to bear in mind that product concentration profiles will strongly depend

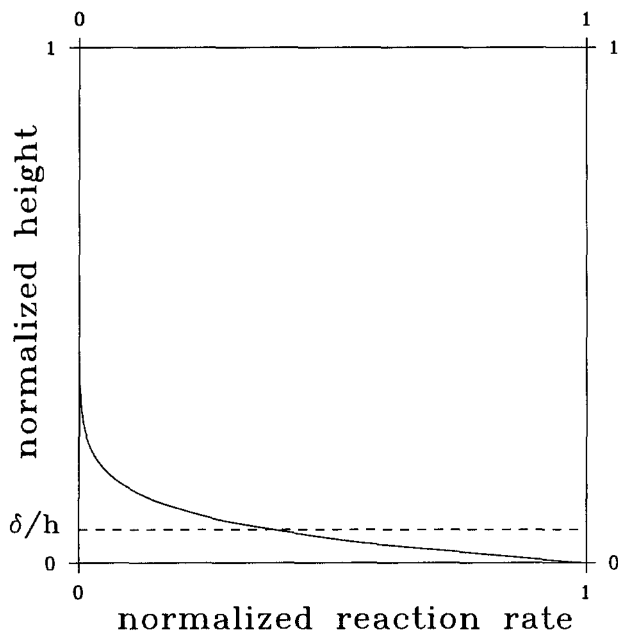

Fig. 2. Normalized reaction rate as function of the normalized height in the reactor with first-order approximation of the chemical boundary layer, *i.e.*, constant reaction rate in boundary layer of width δ. The full line is the exact behavior, the dotted line represents the first model.

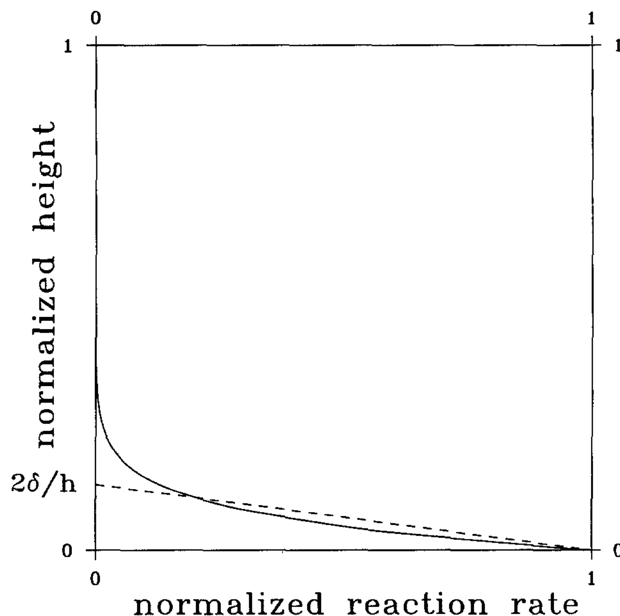

Fig. 3. Normalized reaction rate as function of the normalized height in the reactor with second-order approximation of the chemical boundary layer, *i.e.*, rate varying linearly with height in boundary layer of width 2δ. The full line is the exact behavior, the dotted line represents the second model.

on the model used in the calculations and therefore will differ in the two cases. We will make use of the notation of part I, in which we denote by $J_{D,Q}$ the total diffusional flux of component Q in the vertical direction, by $J_{F,Q}$ the flux component Q because of forced flow in the horizontal direction, and by $[Q]$ the concentration of species Q.

Reversible reactions in the gas-phase-reaction-limited regime.—In part I we analyzed the situation for irreversible reaction in the gas phase kinetics limited regime, and a solution was given for the corresponding deposition rate. A new situation arises when reversible reactions of the type

$$R \underset{k_2}{\overset{k_1}{\rightleftarrows}} P \qquad [b]$$

are considered. When it is assumed that deposition takes place because of adsorption of P onto the substrate, whereas the sticking coefficient of R is zero, one can quite easily give the flux equations for reactant R and product P, *viz.*

$$J_{F,R}|_0^h = J_{D,R}|_0^h - \int_0^h k_1[R]dy + \int_0^h k_2[P]dy = - \int_0^h k_1[R]dy + \int_0^h k_2[P]dy \qquad [4]$$

and

$$J_{F,P}|_0^h = J_{D,P}|_0^h + \int_0^h k_1[R]dy - \int_0^h k_2[P]dy = - J_{D,P}(0) + \int_0^h k_1[R]dy - \int_0^h k_2[P]dy \qquad [5]$$

as follows from the integration of the corresponding continuity equations, thereby accounting for the remarks on adsorption of the different species. Using the concept of the boundary layer, the two-source term of the right-hand side of both equations can be written as $k_1[R]\delta_1$ and $k_2[P]\delta_2$, respectively, where the magnitudes of δ_1 and δ_2 are determined by the respective activation energies E_1 and E_2, as given in Eq. [3]. The use of Eq. [3] for the determination of δ_2 is only allowed when the T-dependence of k_2 is large, as is deduced in part I (Eq. 24, 25, and 57).

This gives

$$J_{F,R}|_0^h = -k_{1,T_s}[R_{T_s}]\delta_1 + k_{2,T_s}[P_{T_s}]\delta_2 \qquad [6]$$

and

$$J_{F,P}|_0^h = -J_{D,P}(0) + k_{1,T_s}[R_{T_s}]\delta_1 - k_{2,T_s}[P_{T_s}]\delta_2 \qquad [7]$$

The forced fluxes $J_{F,R}$ and $J_{F,P}$ at the left-hand side of these equations, which flow through a cross section given by $w \times h$, can also be split up into forced fluxes through cross-sectional areas $w \times \delta$ and $w \times (h - \delta)$, where w is the width of the reactor. Here one must be careful which δ should be used. This will be shown below.

In the following one will distinguish between three different cases, *viz.*, $\delta_1 = \delta_2$, $\delta_1 < \delta_2$, and $\delta_1 > \delta_2$, as determined by the magnitude of the respective activation energies, E_1 and E_2. In the following we will shortly discuss the differences in these three cases. Especially it will be shown that the relative magnitude of the two chemical reaction boundary layers has a strong influence on the general form of the derived deposition rate equations.

Solutions of the flux equations, model 1.—Case 1, $\delta_1 = \delta_2$.—Because only one chemical reaction boundary layer thickness appears in this case, see Fig. 4, indicating that forward and back reaction will take place in the same region in the reactor, the splitting-up of the fluxes $J_{F,R}|_0^h$ and $J_{F,P}|_0^h$, because of flow through boundary layers and bulk of the gas phase, is performed without any problem. From part I it follows that for this case $J_{F,R}|_\delta^h = -J_{D,R}(\delta)$ and $J_{F,P}|_\delta^h = -J_{D,P}(\delta)$, so we obtain

$$J_{F,R}|_0^\delta = J_{D,R}(\delta) - k_{1,T_s}[R_{T_s}]\delta + k_{2,T_s}[P_{T_s}]\delta \qquad [8]$$

and

$$J_{F,P}|_0^\delta = J_{D,P}(\delta) - J_{D,P}(0) + k_{1,T_s}[R_{T_s}]\delta - k_{2,T_s}[P_{T_s}]\delta \qquad [9]$$

with $\delta = \delta_1 = \delta_2$

The complete temperature-dependent flux Eq. [4] and [5] now have been reduced to flux equations within the boundary layer at a temperature equal to the substrate temperature.

In order to find the deposition rate of P, one must return to the original differential equations, *i.e.*, the equivalent continuity equations in the boundary layer. They can be written from Eq. [8] and [9], as shown in Eq. [10] and [11]. For reaction rate-limited growth we can put the left-hand

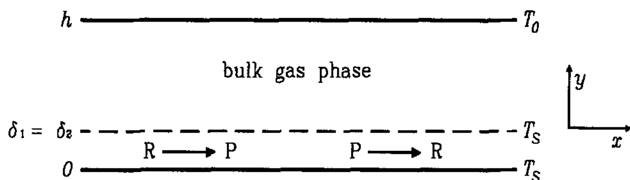

Fig. 4. Schematic view of the different reaction regions in a horizontal CVD reactor for case 1, $\delta_1 = \delta_2$, indicating the reactions proceeding in the boundary layers. Note that no reaction occurs in the bulk of the gas phase.

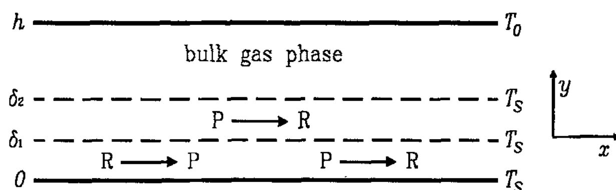

Fig. 5. Schematic view of the different reaction regions in a horizontal CVD reactor for case 2, $\delta_2 > \delta_1$, indicating the reactions proceeding in the boundary layers. Note that no reaction occurs in the bulk of the gas phase.

sides equal to zero for reasons given in part I, *viz.*, $v_x \approx 0$, $\partial[Q]/\partial y \approx 0$, whereas the differential fluxes are replaced by Fick's law. Hence

$$0 = D_{R,T_s} \frac{\partial^2[R]}{\partial y^2} - k_{1,T_s}[R] + k_{2,T_s}[P] \quad [10]$$

and

$$0 = D_{P,T_s} \frac{\partial^2[P]}{\partial y^2} + k_{1,T_s}[R] - k_{2,T_s}[P] \quad [11]$$

for $y \in (0, \delta)$

In these equations D_{Q,T_s} equals the diffusion constant of species Q at the substrate temperature. One may calculate now the deposition rate of P in the usual way by solving these differential equations for $[P(y)]$ and $[R(y)]$ with the following boundary conditions

$$D_{R,T_s} \frac{\partial[R]}{\partial y}\bigg|_0 = 0 \qquad D_{P,T_s} \frac{\partial[P]}{\partial y}\bigg|_0 = k_s[P]_{y=0}$$
$$[R]_{y=\delta} = [R_{T_s}] \qquad D_{P,T_s} \frac{\partial[P]}{\partial y}\bigg|_\delta = 0 \quad [12]$$

where k_s is the first-order rate constant for adsorption and/or surface reaction for species P. The last boundary condition is introduced to depict the behavior of the concentration of P in the case of a fully developed $[P]$ profile in the bulk of the gas phase.

Using the fact that in the gas phase reaction-limited regime the forward chemical reaction rate must be small as compared to diffusional processes, one finds for the deposition rate

$$\underline{r} = k_1 \sqrt{\frac{D_P}{k_2}}[R_{T_s}] \frac{\sinh\left(\sqrt{\frac{k_2}{D_P}}\,\delta\right)}{\cosh\left(\sqrt{\frac{k_2}{D_P}}\,\delta\right) + \frac{\sqrt{k_2 D_P}}{k_s}\sinh\left(\sqrt{\frac{k_2}{D_p}}\,\delta\right)} \quad [13]$$

in which the rate parameters and the diffusion constant have to be evaluated at the susceptor temperature. The reagent concentration $[R_{T_s}]$ has to be calculated at the substrate temperature as well, but care must be taken of thermal diffusion effects and of the mass conservation of the carrier gas, as discussed in part I.

Case 2, $\delta_1 < \delta_2$.—Now there are three different regions in the reactor, *i.e.*, bulk gas phase where no reaction takes place, the boundary layer δ_1 where both forward and back reactions proceed, and an intermediate region from δ_1 to δ_2 where only the back reactions will occur. The situation is sketched in Fig. 5. The foregoing implies that we have to split up the flux Eq. [4] and [5] as given in Eq. [14] and [15].

$$J_{F,R}|_0^{\delta_1} = J_{D,R}(\delta_1) - k_{1,T_s}[R_{T_s}]\delta_1 + k_{2,T_s}[P_{T_s}]\delta_2 \quad [14]$$

and

$$J_{F,P}|_0^{\delta_2} = J_{D,P}(\delta_2) - J_{D,P}(0) + k_{1,T_s}[R_{T_s}]\delta_1 - k_{2,T_s}[P_{T_s}]\delta_2 \quad [15]$$

The deposition rates of P follows by solving the appropriate continuity Eq. [16] and [17], which may be deduced easily from Eq. [14] and [15] after equating $J_{F,R}|_0^{\delta_1}$ and $J_{F,P}|_0^{\delta_2}$ to zero

$$0 = D_{R,T_s} \frac{\partial^2[R]}{\partial y^2} - k_{1,T_s}[R] + k_{2,T_s}[P] \quad [16]$$

for $y \in (0, \delta_1)$ and

$$0 = D_{P,T_s} \frac{\partial^2[P]}{\partial y^2} + k_{1,T_s}[R](1 - S_{\delta_1}(y)) - k_{2,T_s}[P] \quad [17]$$

for $y \in (0, \delta_2)$ with boundary conditions

$$D_{R,T_s} \frac{\partial[R]}{\partial y}\bigg|_0 = 0 \qquad D_{P,T_s} \frac{\partial[P]}{\partial y}\bigg|_0 = k_2[P]_{y=0}$$
$$[R]_{y=\delta_1} = [R_{T_s}] \qquad D_{P,T_s} \frac{\partial[P]}{\partial y}\bigg|_{y=\delta_2} = 0 \quad [18]$$

Here $S_{\delta_1}(y)$ is the unit step functions, *i.e.*, $S_{\delta_1} = 1$ for $y \geq \delta_1$; note the difference in boundary conditions in δ_1 and δ_2!

In the completely gas reaction-limited regime—when k_1 is almost vanishingly small as compared to the diffusional processes—the deposition rate appears to be given by

$$\underline{r} = k_1 \sqrt{\frac{D_P}{k_2}}[R_{T_s}] \frac{\sinh\left(\sqrt{\frac{k_2}{D_P}}\,\delta_2\right) - \sinh\left(\sqrt{\frac{k_2}{D_P}}\right)(\delta_2 - \delta_1)}{\cosh\left(\sqrt{\frac{k_2}{D_P}}\,\delta_2\right) + \frac{\sqrt{k_2 D_P}}{k_s}\sinh\left(\sqrt{\frac{k_2}{D_P}}\,\delta_2\right)} \quad [19]$$

with values of the rate constants, the diffusion coefficient, and the reactant concentration evaluated at susceptor temperature. As is to be expected, one can easily show that Eq. [19] reduces to Eq. [13] for equal boundary layer thicknesses δ_1 and δ_2.

Case 3, $\delta_1 > \delta_2$.—Similarly to the second case, there are three different reaction regions in the reactor, as is depicted in Fig. 6: bulk gas phase, which is the region where no reaction takes place, the boundary layers of reaction [2] with thickness δ_2, where both forward and back reactions proceed, and the region with thickness $\delta_1 - \delta_2$, between the boundary layer of the back reactions and the bulk gas phase. In this last region only the forward reaction occurs.

For this case the flux equations can be shown to be completely similar to the flux equations of case 2, Eq. [14] and [15]. However, the equivalent continuity equations within

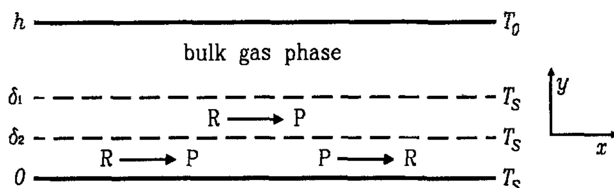

Fig. 6. Schematic view of the different reaction regions in a horizontal CVD reactor for case 3, $\delta_1 > \delta_2$, indicating the reactions proceeding in the boundary layers. Note that no reaction occurs in the bulk of the gas phase.

the reaction boundary layer δ_1 appear to be different from Eq. [16] and [17], as may be deduced readily

$$0 = D_{R,T_s}\frac{\partial^2[R]}{\partial y^2} - k_{1,T_s}[R] + k_{2,T_s}[P](1 - S_{\delta_2}(y)) \quad [20]$$

$$0 = D_{P,T_s}\frac{\partial^2[P]}{\partial y^2} + k_{1,T_s}[R] - k_{2,T_s}[P](1 - S_{\delta_2}(y)) \quad [21]$$

Solving both equations with the appropriate boundary conditions, Eq. [22]

$$D_{R,T_s}\left.\frac{\partial[R]}{\partial y}\right|_0 = 0 \qquad D_{P,T_s}\left.\frac{\partial[P]}{\partial y}\right|_0 = k_s[P]_{y=0}$$
$$[R]_{y=\delta_1} = [R_{T_s}] \qquad D_{P,T_s}\left.\frac{\partial[P]}{\partial y}\right|_{y=\delta_1} = 0 \quad [22]$$

one may find the deposition rate of P. Under the supposition that the forward reaction is sufficiently slow as compared to diffusional processes, it follows that

$$\underline{r} = k_1\sqrt{\frac{D_P}{k_2}}[R_{T_s}] \frac{\sinh\left(\sqrt{\frac{k_2}{D_P}}\delta_2\right) + \left(\sqrt{\frac{k_2}{D_P}}\right)(\delta_1 - \delta_2)}{\cosh\left(\sqrt{\frac{k_2}{D_P}}\delta_2\right) + \frac{\sqrt{k_2D_P}}{k_s}\sinh\left(\sqrt{\frac{k_2}{D_P}}\delta_2\right)} \quad [23]$$

where all constants and the concentration of the reactant R have to be calculated at susceptor temperature. Also, in this case the limiting form of Eq. [23] for δ_1 approaching δ_2 equals Eq. [13], the rate equation derived for equal chemical boundary layer widths.

Three other interesting limiting cases may be obtained from rate expressions [13], [19], and [23]

i.) As expected, one regains in the limiting process of very small values of k_2 (or δ_2)-or better when the rate of the back reaction is much smaller than the diffusion out of the boundary layer

$$\underline{r} = k_1[R_{T_s}]\delta_1 \quad [24]$$

the deposition rate equation for a unidirectional reaction, as derived in part I. The same expression can be derived for case 2 for the case of very small values of δ_1 together with large values of k_s.

ii.) For very large values of k_2 and/or δ_2, however, *i.e.*, when the rate of the back reaction is larger than the diffusion rate of the boundary layer, it can be shown that all three rate equations reduce to Eq. [25]

$$\underline{r} = k_1\sqrt{\frac{D_P}{k_2}}[R_{T_s}]\frac{1}{1 + \frac{\sqrt{k_2D_P}}{k_s}} \quad [25]$$

in which no reference to chemical boundary layers is present anymore. In this relation the role of the boundary layer widths has been taken by $\sqrt{D_P/k_2}$, the diffusion length of product P, which in fact is the mean distance a product molecule can traverse by diffusion through a boundary layer before reaction back to reactant R. If in this case, also, the surface reaction step becomes very fast, we arrive at

$$\underline{r} = k_1\sqrt{\frac{D_P}{k_2}}[R_{T_s}] \quad [26]$$

which relation already was obtained by Moffat and Jensen (3) in their study of silicon deposition from silane.

iii.) When the rate of the surface reaction is much smaller than the rate of the back reaction, we end up, for all cases, with

$$\underline{r} = k_s\frac{k_1}{k_2}[R_{T_s}] \quad [27]$$

an equation describing the adsorption, and possibly concomitant surface reaction, of product P in equilibrium with reactant R at gas temperature T_s. Case [26] and [27] describe the situations where either the reactions in the gas phase are rate-limiting or surface reactions are the slowest process.

Solution of the flux equations, model 2.—Having solved the flux equations for the simple model of reaction rate constants, independent of height within the boundary layers, we now will proceed by using linearly variable rate parameters, k_i, *viz.*

$$k_1 = k_{1,T_s}(1 - y/2\delta_1) \quad [28]$$

and

$$k_2 = k_{2,T_s}(1 - y/2\delta_2) \quad [29]$$

in boundary layers of width $2\delta_1$ and $2\delta_2$, respectively. The temperature in these boundary layers will be taken to be approximately constant as far as reactant concentration and diffusion coefficients are concerned, stressing the far stronger temperature dependence of rate constants as compared to the variation of the other parameters in the reactor system. In this way the reaction rate appears to be higher in the lower region of the reaction boundary layer near the hot susceptor, in accordance with the practical situation. Proceeding along the lines of model 1, it now is possible to write down the continuity equations that correspond with cases 1, 2, and 3, *i.e.*, by taking care in Eq. [10,

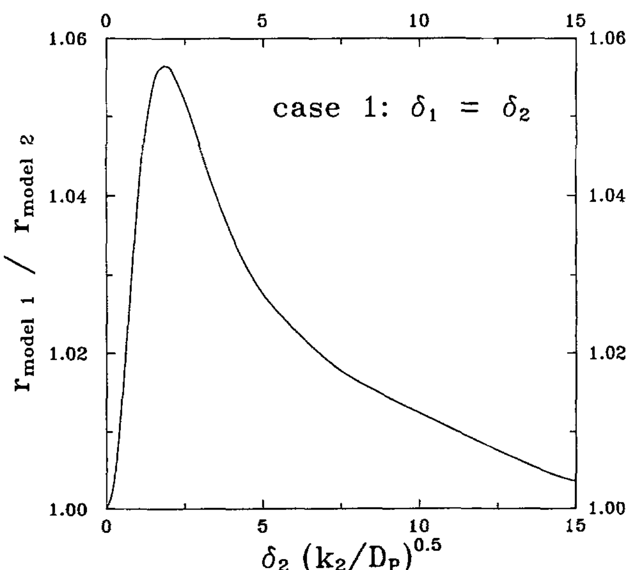

Fig. 7. Maximum ratio of deposition rates calculated by means of model 1 and model 2 for case 1, $\delta_1 = \delta_2$, as a function of $\delta_2 \cdot \sqrt{k_2/D_P}$.

11, 16, 17, 20, 21] of the height variation of the rate constants and changing the boundaries δ_1 and δ_2 in $2\delta_1$ and $2\delta_2$, respectively. With the assumption of a sufficiently slow forward reaction as compared to diffusional processes—thus assuming no limitation of gas phase transport—very complicated solutions for the rate equations can be obtained after a lot of tedious mathematics. Equations [30]-[32] show the expressions for the case that the rate for adsorption and/or surface reaction is larger than the rate for the back reaction in the boundary layer, *i.e.*, for the completely gas phase kinetics-limited regime. One finds for case 1, $\delta_1 = \delta_2$

$$\underline{r} = k_1 \sqrt{\frac{D_P}{k_2}}[R_{T_s}] \left\{ \frac{I_{2/3}}{I_{-1/3}} \bigg|_{2/3\eta} \right\} \quad [30]$$

for case 2, $\delta_1 < \delta_2$

$$\underline{r} = k_1 \sqrt{\frac{D_P}{k_2}}[R_{T_s}] \left\{ \frac{\delta_2}{\delta_1} \left[\frac{I_{2/3}}{I_{-1/3}} \bigg|_{2/3\eta} \left[1 + \pi\eta^{2/3}\left(1 - \frac{\delta_1}{\delta_2}\right) H_i(\eta^{2/3}) \right.\right.\right.$$

$$\left. - \pi\eta^{1/3}\left(1 - \frac{\delta_1}{\delta_2}\right) H_i'(\eta^{2/3}) \right] + \frac{\delta_2}{\delta_1} \frac{\left\{ I_{-2/3} - \frac{I_{1/3}I_{2/3}}{I_{-1/3}} \right\}_{2/3\eta}}{\left\{ I_{-2/3} - \frac{I_{1/3}I_{2/3}}{I_{-1/3}} \right\}_{2/3\eta(1-\delta_1/\delta_2)^{3/2}}}$$

$$\cdot \left\{ \pi\eta^{1/3} H_i'\left(\eta^{2/3}\left(1 - \frac{\delta_1}{\delta_2}\right)\right) - \frac{I_{2/3}}{I_{-1/3}} \bigg|_{2/3\eta(1-\delta_1/\delta_2)^{3/2}} \right.$$

$$\left.\left.\left. \cdot \left\{ \frac{1}{\sqrt{1 - \frac{\delta_1}{\delta_2}}} + \sqrt{1 - \frac{\delta_1}{\delta_2}}\, \pi\eta^{2/3} H_i\left(\eta^{2/3}\left(1 - \frac{\delta_1}{\delta_2}\right)\right) \right\} \right\} \right\} \quad [31]$$

and for case 3, $\delta_1 > \delta_2$

$$\underline{r} = k \sqrt{\frac{D_P}{k_2}}[R_{T_s}] \left\{ 3^{1/3}\Gamma\left(\frac{4}{3}\right)\eta \left\{ \frac{\eta^{2/3}}{2}\left(1 - \frac{\delta_2}{\delta_1}\right)\left(\frac{\delta_1}{\delta_2} - 1\right) \right.\right.$$

$$\left. + \pi\left(1 - \frac{\delta_2}{\delta_1}\right) Gi'(0) \right\} \left\{ I_{-2/3} - \frac{I_{1/3}I_{2/3}}{I_{-1/3}} \right\}_{2/3\eta}$$

$$+ \left\{ \frac{\delta_2}{\delta_1} + \pi\eta^{2/3}\left(1 - \frac{\delta_2}{\delta_1}\right) Gi(\eta^{2/3}) \right\} \frac{I_{2/3}}{I_{-1/3}} \bigg|_{2/3\eta}$$

$$\left. - \pi\eta^{1/3}\left(1 - \frac{\delta_2}{\delta_1}\right) Gi'(\eta^{2/3}) \right\} \quad [32]$$

with

$$\eta = \frac{2\delta_2}{\sqrt{D_P/k_2}} \quad [33]$$

the ratio of the total boundary layer width for the back reaction and the diffusion length of product P. In these equations, I_j are modified Bessel functions of the first kind and of order j, whereas G_i, G_i', H_i, and H_i' are functions related to Airy functions and integrals of these as defined by Abramowitz and Stegun (11). As usual, all variables have to be evaluated at susceptor temperatures.

In normal practice, equations such as [30]-[32] are very inconvenient and difficult to handle, but it can be shown easily that in the limits of very small and of very large values of η, *i.e.*, for very small and very large values of k_2, the rate constant of the back reaction, one regains the rate expressions

$$\underline{r} = k_1[R_{T_s}]\delta_1 \quad [34]$$

and

$$\underline{r} = k_1 \sqrt{\frac{D_P}{k_2}}[R_{T_s}] \frac{1}{1 + \frac{\sqrt{k_2 D_P}}{k_s}} \quad [35]$$

respectively. Equation [34], obtained for very small values of k_2, is equal to the expression for an irreversible reaction given in part I, whereas Eq. [35], derived for very large values of k_2, is identical to Eq. [25], which was derived in the block-profile model for the chemical boundary layer.

When the rate of the surface reaction is smaller than the rate of the back reaction, complex equations can be derived, similar to Eq. [30]-[33], which upon simplification end up as

$$r = k_s \frac{k_1}{k_2}[R_{T_s}] \quad [36]$$

In general one can prove that reaction rates calculated from expression derived with model 2 will not differ more than about 20% from rates computed by means of model 1. Figure 7, *e.g.*, shows the maximum ratio of deposition rates (model 1/model 2) for case 1, $\delta_1 = \delta_2$ as a function of $\delta_2\sqrt{k_2/D_P}$. In this case the difference between the two models is even smaller than 6%. Hence, as boundary layer calculations are always approximate in nature, it seems appropriate to avoid the mathematical complexities connected with the introduction of non-constant rate parameters in this type of calculation.

Conclusion

In part I of this series an analysis was presented which allowed us to derive semiquantitative deposition rate equations in horizontal CVD reactors when the deposition process is a product of an activated unidirectional chemical reaction in the gas phase. In the present paper, we have shown that, using the already developed notion of chemical boundary layers, it is possible to arrive at analytical rate expressions for the CVD process in which the deposition is governed by an activated, reversible gas-phase reaction.

Two models for the chemical boundary layer were considered in this context, one with constant and one with linearly varying reaction rate parameters within the boundary layers. We found that the obtained results only slightly or even insignificantly depend on the interpretation one has to make within the reaction boundary layer concept. Therefore it seems appropriate to use only the most simple boundary-layer model, *i.e.*, a block profile, for the reaction rate constants as far as the calculation of deposition rates is concerned. Although we did not discuss in this paper the influence of bulk gas-phase transport on the deposition rates, it can be readily accounted for, as is shown by Van Stark *et al.* (12) for the deposition of Si from SiH_4 and for the doping of GaAs with silane as dopant precursor. In a next series of papers the concept of chemical reaction boundary layers will be used to describe more complex processes in the modeling of growth and doping of semiconductors (13-15).

Manuscript submitted Nov. 7, 1989; revised manuscript received June 4, 1990.

The University of Nijmegen assisted in meeting the publication costs of this article.

REFERENCES

1. M. E. Coltrin, R. J. Kee, and J. A. Miller, *This Journal*, **133**, 1206 (1986).
2. J. Ouazzani, K.-C. Chiu, and F. Rosenberger, *J. Cryst. Growth*, **91**, 479 (1988).
3. H. K. Moffat and K. F. Jensen, *This Journal*, **135**, 459 (1988).
4. M. Tirtowidjojo and R. Pollard, *J. Cryst. Growth*, **98**, 420 (1989).

5. J. Bloem and L. J. Giling, in "Current Topics in Material Science," Vol. 1, E. Kaldis, Editor, pp. 147-342, North-Holland Publishing Company, Amerstdam (1987).
6. W. G. J. H. M. van Sark, G. Janssen, M. H. J. M. de Croon, and L. J. Giling, *Semicond. Sci. Technol.*, **5**, 16 (1990).
7. *Ibid.*, 36
8. M. H. J. M. de Croon and L. J. Giling, *This Journal*, **137**, 2867 (1990).
9. J. van de Ven, G. M. J. Rutten, M. J. Raaijmakers, and L. J. Giling, *J. Cryst. Growth*, **76**, 352 (1986).
10. R. B. Bird, W. E. Stewart, and E. N. Lightfoot, "Transport Phenomena," pp. 249-260, John Wiley & Sons, New York (1960).
11. M. Abramowitz and I. A. Stegun, "Handbook of Mathematical Functions," pp. 446-452, Dover Publications, New York (1970).
12. W. G. J. H. M. van Sark, M. H. J. M. de Croon, G. Janssen, and L. J. Giling, *Semicond. Sci. Technol.*, **5**, 291 (1990).
13. P. R. Hageman, X. Tang, M. H. J. M. de Croon, and L. J. Giling, *J. Cryst. Growth*, **98**, 249 (1989).
14. M. H. J. M. de Croon and L. J. Giling, *Prog. Crystal Growth and Charact.*, **19**, 125 (1989).
15. M. H. J. M. de Croon and L. J. Giling, To be published.

Anisotropic Etching of Crystalline Silicon in Alkaline Solutions

I. Orientation Dependence and Behavior of Passivation Layers

H. Seidel

Messerschmitt-Bölkow-Blohm GmbH, D-8000 Munich 80, Germany

L. Csepregi

Fraunhofer-Institut für Festkörpertechnologie, D-8000 Munich 60, Germany

A. Heuberger

Fraunhofer-Institut für Mikrostrukturtechnik, D-1000 Berlin 33, Germany

H. Baumgärtel

Institut für Physikalische Chemie, Freie Universität Berlin, D-1000 Berlin 33, Germany

ABSTRACT

The anisotropic etching behavior of single-crystal silicon and the behavior of SiO_2 and Si_3N_4 in an ethylenediamine-based solution as well as in aqueous KOH, NaOH, and LiOH were studied. The crystal planes bounding the etch front and their etch rates were determined as a function of temperature, crystal orientation, and etchant composition. A correlation was found between the etch rates and their activation energies, with slowly etching crystal surfaces exhibiting higher activation energies and vice versa. For highly concentrated KOH solutions, a decrease of the etch rate with the fourth power of the water concentration was observed. Based on these results, an electrochemical model is proposed, describing the anisotropic etching behavior of silicon in all alkaline solutions. In an oxidation step, four hydroxide ions react with one surface silicon atom, leading to the injection of four electrons into the conduction band. These electrons stay localized near the crystal surface due to the presence of a space charge layer. The reaction is accompanied by the breaking of the backbonds, which requires the thermal excitation of the respective surface state electrons into the conduction band. This step is considered to be rate limiting. In a reduction step, the injected electrons react with water molecules to form new hydroxide ions and hydrogen. It is assumed that these hydroxide ions generated at the silicon surface are consumed in the oxidation reaction rather than those from the bulk electrolyte, since the latter are kept away from the crystal by the repellent force of the negative surface charge. According to this model, monosilicic acid $Si(OH)_4$ is formed as the primary dissolution product in all anisotropic silicon etchants. The anisotropic behavior is due to small differences of the energy levels of the backbond surface states as a function of the crystal orientation.

Anisotropic etchants for crystalline silicon have been known for a long time (1-3). Their first applications included the etching of V-grooves on <100> silicon or U-grooves on <110> silicon, in order to fabricate MOS transistors for high power and high current densities (4). Increasing attention has been paid to this etching technology, after recognizing its unique capabilities for micromachining three-dimensional structures (5-9). Due to the strong dependence of the etch rate on crystal direction and on dopant concentration, a large variety of silicon structures can be fabricated in a highly controllable and reproducible manner. Typical structures include thin membranes, deep and narrow grooves, and cantilevers with single or double sided suspension. Important fields of application include the fabrication of passive mechanical elements, sensors, and actuators, as well as micro-optical components (8, 10). Among the best known examples are sensors for pressure (8), acceleration (11), and flow (12), as well as ink jet nozzles (13), connectors for optical waveguides (14), and major components of a gas chromatograph (15).

All anisotropic etchants are aqueous alkaline solutions, where the main component can be either organic or inorganic. The first organic system was proposed in 1962 and consisted of hydrazine (N_2H_4) and water with the addition of pyrocatechol ($C_6H_4(OH)_2$) (16). It was shown that pyrocatechol is not a necessary component, and might well be omitted (2). Experiments were made with iso-2-propyl alcohol as a third component, which was shown to act as a moderator (3). In a later work, hydrazine was substituted by ethylenediamine ($NH_2(CH_2)_2NH_2$), which is more stable and less toxic than the former (2).

Purely inorganic aqueous solutions of KOH and NaOH have been known to etch silicon anisotropically for a long time (1). A different system with improved etching behavior was obtained by the addition of isopropyl alcohol (17).